D. Laksameethanasan, S. S. Brandt, and P. Engelhardt. 2006. A three-dimensional Bayesian reconstruction method with the point spread function for micro-rotation sequences in wide-field microscopy. In: Proceedings of the 3rd IEEE International Symposium on Biomedical Imaging: From Nano to Macro (ISBI 2006). Arlington, VA, USA. 6-9 April 2006, pages 1276-1279.

# A THREE-DIMENSIONAL BAYESIAN RECONSTRUCTION METHOD WITH THE POINT SPREAD FUNCTION FOR MICRO-ROTATION SEQUENCES IN WIDE-FIELD MICROSCOPY

*D. Laksameethanasan*[1], *S. S. Brandt*[1], *P. Engelhardt*[1,2]

[1]Laboratory of Computational Engineering, Helsinki University of Technology, P.O. Box 9203, FI-02015 TKK, Finland

[2]Haartman Institute, Department of Pathology and Virology, University of Helsinki, P.O. Box 21, FI-00014 University of Helsinki, Finland

## ABSTRACT

In this paper, we present a three-dimensional (3D) reconstruction algorithm for light microscopy supplied with a micro-rotation device. In contrast to the traditional optical sectioning techniques where the focal plane is shifted along the optical axis, in micro-rotation imaging, the object rotates where the focal plane is kept in a fixed position. Our reconstruction algorithm is based on Bayesian inversion theory where the imaging model is described by the 3D point spread function (PSF). The results show that the approach is promising for 3D reconstruction of rotating objects in wide-field light microscopy, as an improvement for the effective 3D resolution is provided.

## 1. INTRODUCTION

Three-dimensional (3D) fluorescence imaging of individual live cells is an essential tool for cellular biology. Previously, 3D reconstructions have been computed by optical sectioning ($z$-stacking) techniques in fluorescence microscopy [1, 2]. The 3D reconstruction is recorded as a stack of 2D images by shifting the focal plane along the optical axis ($z$-axis). Due to the out-of-focus blur, the image stack is restored by deconvolution techniques. However, the z-stacking techniques have limited resolution, especially along the optical axis.

By the novel micro-rotation technique [3, 4], cells are rotated on a fixed focal plane. Instead of moving the focal plane along the optical axis, dielectric fields rotate the cell approximately around a single axis parallel to the focal plane. In this way, the effective 3D resolution level [5] can be significantly improved. The method is primarily used for inspecting the interior structure of objects, such as non-adherent live cells in suspension. The ideal geometrical setting of the method is illustrated in Figure 1.

In this paper, we propose a 3D reconstruction method, based on Bayesian inversion theory, and test it with a micro-rotating image set. The Bayesian inversion is a statistically sound approach for solving inverse problems for a selected noise model where a priori knowledge of the object can be taken into account. The Bayesian approach has been successful in many applications such as medical imaging [6], electron tomography [7] and 3D light microscopy with optical sectioning [8].

In the Bayesian model, we use a Gaussian prior function for the object densities and assume white noise in the measurements. The projection model of the wide-field microscope is described by a 3D point spread function, we assume local linearity and shift invariance on the focal plane and take an advantage of the Fast Fourier Transform (FFT) algorithm in computing the forward projection model.

In order to solve a 3D reconstruction problem, like the one we have, the projection directions must be known. The standard approaches for solving the corresponding motion estimation problem, including fiducial and non-fiducial techniques [9, 10], seem difficult for our test data due to the lack of detail of the object. In this work, we use the method of motion recovery without correspondence [11, 12] that better suits for estimating the motion for these kinds of objects.

The paper begins by introducing the forward projection model and its adjoint in Section 2. The statistical setting, providing the solution for the inverse problem, is described in Section 3. The results of reconstructing the micro-rotating set are reported in Section 4. Finally, we discuss and conclude the paper in Section 5.

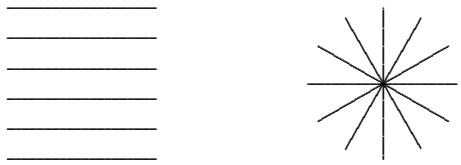

**Fig. 1**. Ideal geometries of optical-sectioning and micro-rotation techniques. Each line represents the focal plane in the object coordinate frame.

## 2. PROJECTION MODEL

In this section, we will present how the measurement plane can be constructed from the 3D object, as the 3D Point Spread Function (PSF) is given. The forward model can be mathematically described by the linear operator $A : C_3 \rightarrow C_2$ such that $m = Af$, where $f \in C_3$ is the piecewise continuous density volume and $m = \{m_i\} \in C_2$ presents the set of piecewise continuous projection images. The forward model is constructed as follows.

As a linear system, a wide-field microscope can be characterized by a 3D PSF which is the response volume for a point source. If the microscope system is shift invariant, the operation by the PSF can be represented by the convolution

$$g_i(\mathbf{r}) = \int_{\mathbb{R}^3} f_i(\mathbf{r}')h(\mathbf{r} - \mathbf{r}')\, d\mathbf{r}' = f_i(\mathbf{r}) * h(\mathbf{r}), \tag{1}$$

where $g_i$ is the blurred volume and $f_i(\mathbf{r}) = R_i f(\mathbf{r})$ is the rotated object density for the $i$th projection, $R_i$ is the rotation operator, $h$ is the point spread function, and $*$ is the convolution operator. We assume that the optical axis is along the $z$-direction. The measurement image $i$ is obtained as the plane corresponding to the focal plane $z = d$; i.e.,

$$m_i(x, y) = g_i(x, y, d). \tag{2}$$

In the minimization problem, we additionally need the adjoint operator $A^* : C_2 \rightarrow C_3$ which describes the construction of a 3D object from the measurement planes by zero-padding, correlation, rotation and superimposing the obtained volumes. In other words, let $\tilde{f} = A^*m$, where $m = \{m_i\} \in C_2$ and $\tilde{f} \in C_3$; we get

$$\tilde{f}(\mathbf{r}) = \sum_i \int_{\mathbb{R}^3} \tilde{g}_i(\mathbf{r}')h(\mathbf{r}' - \mathbf{r})\, d\mathbf{r}', \tag{3}$$

where $\tilde{g}_i(\mathbf{r}) = R_i^*\{m_i(x, y)\delta(z - d)\}$ and $\delta(z)$ is the Dirac-delta function.

Due to linearity of the operator $A$, the discretized model can be represented as a linear system

$$\mathbf{m} = \mathbf{Af}, \tag{4}$$

where $\mathbf{f}$ is a vector of density values (voxels), $\mathbf{m}$ is a vector of all the image measurements (pixels), and the matrix $\mathbf{A}$ is the block Toeplitz matrix representing the 2D convolution operations. In practice, the matrix-vector product can efficiently computed by the FFT algorithm while the 3D interpolation between PSF and rotating object coordinates is required in computing the convolution integrals. For the adjoint operator, the corresponding discretized model is $\tilde{\mathbf{f}} = \mathbf{A}^{\mathrm{T}}\mathbf{m}$.

## 3. BAYESIAN INVERSION

We consider the linear model with additive white Gaussian noise, i.e.,

$$\mathbf{m} = \mathbf{Af} + \mathbf{n}, \tag{5}$$

where $\mathbf{m}$, $\mathbf{f}$ and $\mathbf{n}$ are vectors of random variables.

In Bayesian inversion theory, the complete solution for an inverse problem is represented by the posterior distribution, given by Bayes' formula

$$p(\mathbf{f}|\mathbf{m}) = \frac{p(\mathbf{f})p(\mathbf{m}|\mathbf{f})}{p(\mathbf{m})} \propto p(\mathbf{f})p(\mathbf{m}|\mathbf{f}), \tag{6}$$

where $p(\mathbf{m}|\mathbf{f})$ is the likelihood density, $p(\mathbf{f})$ is the prior density and p($\mathbf{m}$) is a normalization constant. The posterior distribution is often very large dimensional, so an efficient tool for estimating the solution is crucial.

In the paper, we select the maximum a posteriori (MAP) estimate which is obtained from

$$\hat{\mathbf{f}} = \arg\max p(\mathbf{f}|\mathbf{m}). \tag{7}$$

It means that for the given prior density $p(\mathbf{f})$ and the measurement data $\mathbf{m}$, we determine the unknown values $\mathbf{f}$ which are in the best agreement with the model (5).

Assuming zero mean, isotropic Gaussian noise with variance $\sigma_n^2$, the likelihood function is

$$p(\mathbf{m}|\mathbf{f}) \propto \exp\left(-\frac{\|\mathbf{m} - \mathbf{Af}\|^2}{2\sigma_n^2}\right). \tag{8}$$

The next question is how to choose the prior density function $p(\mathbf{f})$. For simplicity, we select the Gaussian, white noise prior with the positivity constraint, i.e.,

$$p(\mathbf{f}) \propto \exp\left(-\frac{\|\mathbf{f}\|^2}{2\sigma_f^2}\right) u(\mathbf{f}), \tag{9}$$

where the step function $u(\mathbf{f})$ equals to one when all the elements in $\mathbf{f}$ are positive; otherwise it is zero.

Inserting (8) and (9) into (6), the computation of MAP (7) implies minimizing

$$\begin{aligned} \hat{\mathbf{f}} &= \arg\min \left\{\|\mathbf{m} - \mathbf{Af}\|^2 + \lambda\|\mathbf{f}\|^2\right\} \\ &= \arg\min \left\{\mathbf{e}^{\mathrm{T}}\mathbf{e}\right\}, \end{aligned} \tag{10}$$

where the vector $\mathbf{e} = (\mathbf{m} - \mathbf{Af}, \sqrt{\lambda}\mathbf{f})^{\mathrm{T}}$ and the regularization parameter $\lambda = \sigma_n^2/\sigma_f^2$. In other words, the higher the noise level $\sigma_n^2$ in the measurements the larger the regularization parameter is required. The statistical estimation problem is hence converted into an optimization problem.

In practice, we compute the MAP-estimates by the trust-region iterative method as implemented in Matlab Optimization Toolbox [13]. As the trust-region algorithm is the second-order iterative method, the minimization requires computing of the operations $\mathbf{J}^{\mathrm{T}}\mathbf{Jy}$, $\mathbf{Jy}$ and $\mathbf{J}^{\mathrm{T}}\mathbf{y}$, where $\mathbf{J}$ is the Jacobian matrix of the vector $\mathbf{e}$, and $\mathbf{y}$ is a vector. Instead of explicitly creating a huge Jacobian matrix and computing the expensive matrix-vector product, the Jacobian operations can efficiently be computed by the FFT algorithm similarly as explained in Section 2.

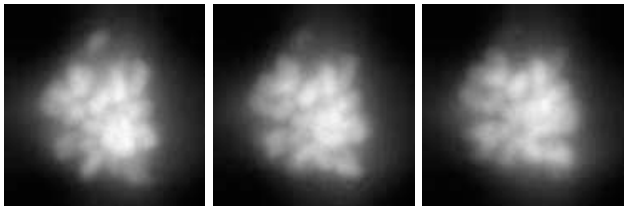

**Fig. 2**. Example images of prophase chromosomes in cell mitosis.

## 4. RESULTS

The proposed method was tested with a micro-rotation set representing a cell mitosis. This set consisted of 90 images, with $195 \times 212$ pixels, obtained by a wide-field light microscope; after the translation correction and the cropping of region of interest, the final size used was $121 \times 121$. By applying the motion estimation method, we found out that there were five complete revolutions with the fundamental period of 18.1 images. Figure 2 shows some example images from the set.

The simulated 3D PSF corresponding to the microscope setup was computed by the SVI Huygens software [14], see Figure 3. The upper row shows the 1D-plot along $x$ and $z$-axis (optical axis) at the center of the PSF; the lower row displays the two 2D-slices of the $xy$-plane (corresponding to the focal plane) and the $yz$-plane.

The full size ($121 \times 121 \times 121$) reconstruction of the mitosis set is illustrated in Figures 4–6. Figure 4 and 5 show the $xz$ and $yz$-slices through the reconstruction while Figure 6 displays a wall-eye stereo-view of the reconstruction. As can be seen, our reconstruction method was successful, even though there seem to be small grain artifacts around the rotation axis ($x$-axis) at the center of $yz$-slice.

## 5. CONCLUSIONS

In this paper, we have proposed a Bayesian method for solving the 3D reconstruction of a rotating object from wide-field light microscope images, assuming that the motion estimates and the PSF are available. We used a Gaussian prior function and assumed white noise in the measurements. The method was experimented with a micro-rotating set of a cell mitosis. The results show that, the complex cell structure can be reconstructed by the method.

In future, there are plenty of things to investigate such as the selection of a more sophisticated prior function and the value for the regularization parameter. These extensions have been intensively investigated with the optical sectioning techniques in the last two decades, while most of them can be directly applied for the new methodology. The computation of the 3D reconstructions with our current implementation is relatively expensive. The computational improvement is hence another topic in the further work.

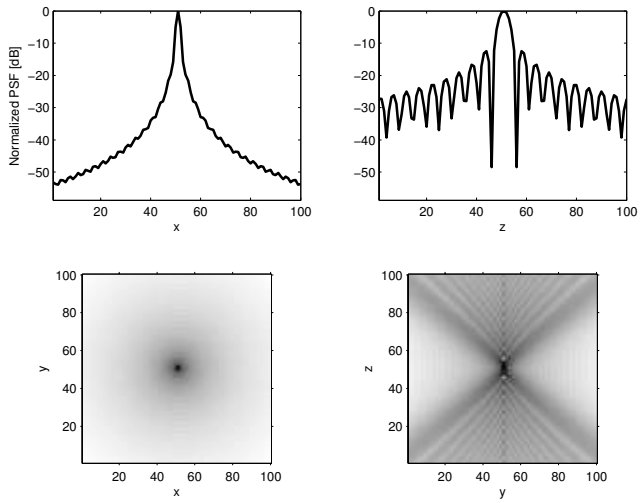


**Fig. 3**. The three-dimensional point spread function.

## 6. ACKNOWLEDGMENT

This work is supported by the European Commission (NEST 2005 programme) in consortium AUTOMATION (Coordinator S.L. Shorte, Institut Pasteur, Paris). The "Micro-rotation movies" are from the Plateforme d'Imagerie Dynamique (Institut Pasteur, Paris), and were recorded by S.L. Shorte and G. Langsley. We additionally thank O. Renaud, Institut Pasteur, for providing the simulated PSF for testing. The movies are openly available for viewing at:
http://www.pfid.org/AUTOMATION/galleryhome/.

## 7. REFERENCES

[1] D. Agard, Y. Hiraoka, P. Shaw, and J. Sedat, "Fluorescence microscopy in three dimensions," Meth. Cell. Biol., vol 30, pp. 353-377, 1989.

[2] A. Erhardt, G. Zinser, D. Komitowski, and J. Billie, "Reconstructing 3-D light-microscopic images by digital image processing," in Applied Optics, vol 24(2), pp. 194-200, 1985.

[3] R. Lizundia, L. Sengmanivong, J. Guergnon, J. Wang., T. Mueller, T. Schnelle, B. Chalmond, G. Langsley and S.L. Shorte, "Using micro-rotation imaging to study JNK-mediated cell survival in Theileria parva-infected B-lymphocytes", ISSN 0031-1820, pp. 629-636, 2005.

[4] J. Korlach, C. Reichle, T. Mueller, T. Schnelle and W.W. Web, "Trapping, deformation, and rotation of giant unilamellar vesicles in octode dielectrophoretic field cage", Biophysical Journal, vol 89, pp. 554-562, 2005.

[5] P.J. Shaw, D.A. Agard, Y. Hirakoa and J.W. Sedat, "Tilted view reconstruction in optical microscopy: three

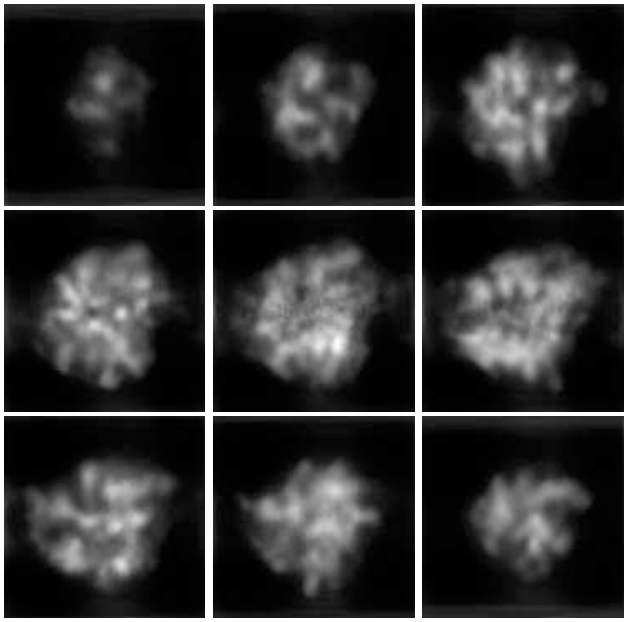

**Fig. 4**. Example $xz$-slices of the reconstruction.

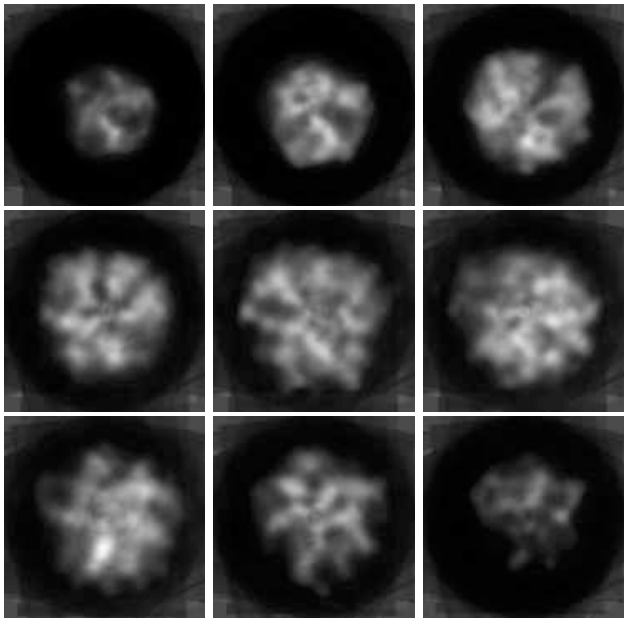

**Fig. 5**. Example $yz$-slices of the reconstruction.

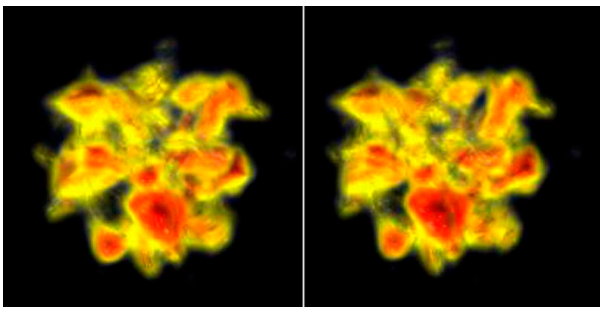

**Fig. 6**. 3D wall-eye stereo-view of the reconstruction.


dimensional reconstruction of Drosophila melanogaster embryo nuclei," Biophys. J. 55, 101110, 1989.

[6] V. Kolehmainen, S. Siltanen, S. Järvenpää, J.P. Kaipio, P. Koistinen, M. Lassas, J. Pirttilä and E. Somersalo, "Statistical inversion for medical X-ray tomography with few radiographs II: Application to dental radiology," Phy. Med. Bio. 48, pp. 1465-1490, 2003.

[7] U. Skoglund, L.G. fverstedt, R. Burnett, and G. Bricogne, "Maximum-entropy three-dimensional reconstruction with deconvolution of the contrast transfer function: a test application with adenovirus," J. Struc. Bio., vol 117, pp. 173-188, 1996.

[8] P.J. Verveer, M.J. Gemkow, T.M. Jovin, "A comparison of image restoration approaches applied to three-dimensional confocal and wide-field fluorescence microscopy," J. Microsc. 193: 50-61, 1999.

[9] S. Brandt, J. Heikkonen, and P. Engelhardt, "Multiphase method for automatic alignment of transmission electron microscope images using markers," J. Struct. Biol., vol 133(1), pp. 10-22, 2001.

[10] S. Brandt, J. Heikkonen, and P. Engelhardt, "Automatic alignment of transmission electron microscope tilt series without fiducial markers," J. Struct. Biol., vol 136(3), pp. 201-213, 2001.

[11] S. Brandt and V. Kolehmainen, "Motion without correspondence from tomographic projections by Bayesian inversion theory," In Proceedings of the IEEE Computer Society Conference on Computer Vision and Pattern Recognition (CVPR), vol I, pp. 582-587, Washington DC, June 2004.

[12] S. Brandt and M. Mevorah, "Camera Motion Recovery without Correspondence from Micro-Rotation Sets in Wide-Field Light Microscopy," Submitted for publication.

[13] T.F. Coleman and Y. Li, "An Interior, Trust Region Approach for Nonlinear Minimisation Subject to Bounds," SIAM J. Optim., vol 6, pp. 418-445, 1996.

[14] http://www.svi.nl/